

Effect of nitrogen on the optical and transport properties of Ga_{0.48}In_{0.52}N_yP_{1-y} grown on GaAs(001) substrates

Y. G. Hong, A. Nishikawa, and C. W. Tu

Citation: [Applied Physics Letters](#) **83**, 5446 (2003); doi: 10.1063/1.1637148

View online: <http://dx.doi.org/10.1063/1.1637148>

View Table of Contents: <http://scitation.aip.org/content/aip/journal/apl/83/26?ver=pdfcov>

Published by the [AIP Publishing](#)

Articles you may be interested in

Hole traps associated with high-concentration residual carriers in p-type GaAsN grown by chemical beam epitaxy
J. Appl. Phys. **117**, 045712 (2015); 10.1063/1.4906991

Similarities between Ga_{0.48}In_{0.52}N_yP_{1-y} and Ga_{0.92}In_{0.08}N_yAs_{1-y} grown on GaAs (001) substrates
J. Vac. Sci. Technol. B **22**, 1495 (2004); 10.1116/1.1752915

Metal organic vapor phase epitaxial growth of heavily carbon-doped GaAs using a dopant source of CCl₃Br and quantitative analysis of the compensation mechanism in the epilayers
J. Appl. Phys. **93**, 1613 (2003); 10.1063/1.1534377

Annealing behavior of p-type Ga_{0.892}In_{0.108}N_xAs_{1-x} (0 ≤ x ≤ 0.024) grown by gas-source molecular beam epitaxy
Appl. Phys. Lett. **75**, 1416 (1999); 10.1063/1.124711

Photoluminescence investigation of GaInP/GaAs multiple quantum wells grown on (001) and (311) B GaAs surfaces by gas source molecular beam epitaxy
J. Appl. Phys. **83**, 7900 (1998); 10.1063/1.367968

A promotional banner for Applied Physics Reviews. On the left is a thumbnail image of a journal cover for 'AIP Applied Physics Reviews' featuring a diagram of a device structure. The main part of the banner has a blue background with a glowing light effect. The text 'NEW Special Topic Sections' is prominently displayed in white. Below this, it says 'NOW ONLINE' in yellow, followed by 'Lithium Niobate Properties and Applications: Reviews of Emerging Trends' in white. The AIP Applied Physics Reviews logo is in the bottom right corner.

NEW Special Topic Sections

NOW ONLINE
Lithium Niobate Properties and Applications:
Reviews of Emerging Trends

AIP Applied Physics Reviews

Effect of nitrogen on the optical and transport properties of $\text{Ga}_{0.48}\text{In}_{0.52}\text{N}_y\text{P}_{1-y}$ grown on GaAs(001) substrates

Y. G. Hong,^{a)} A. Nishikawa, and C. W. Tu

Department of Electrical and Computer Engineering, University of California at San Diego, La Jolla, California 92093-0407

(Received 6 August 2003; accepted 5 November 2003)

We report gas-source molecular-beam epitaxy of $\text{Ga}_{1-x}\text{In}_x\text{N}_y\text{P}_{1-y}$ grown on GaAs(100) substrates. Nitrogen incorporation dramatically reduces the $\text{Ga}_{1-x}\text{In}_x\text{P}$ band gap. With nitrogen incorporation, the photoluminescence (PL) peak energy exhibits an inverted S-shaped dependence with temperature, and the low-temperature PL spectra exhibit an asymmetric line shape with a low-energy tail. Both indicate the presence of N-related localized states, which dominate the radiative recombination processes at low temperature. N incorporation significantly reduces the free-electron concentration and mobility. The free-electron concentration of N-containing $\text{Ga}_{0.48}\text{In}_{0.52}\text{N}_{0.005}\text{P}_{0.995}$ decreases dramatically with high-temperature annealing (800 °C), from 4.4×10^{18} to $8.0 \times 10^{16} \text{ cm}^{-3}$. This is believed to be due to passivation of Si by N through the formation of Si–N pairs. © 2003 American Institute of Physics. [DOI: 10.1063/1.1637148]

Recently, $\text{Ga}_{0.52}\text{In}_{0.48}\text{P}$ -grown lattice matched to GaAs has received considerable attention due to its device applications, such as high-efficiency tandem solar cells¹ and heterojunction bipolar transistors (HBTs).² Nitrogen incorporation in III–V compound semiconductors results in a large band-gap bowing,³ which is due to lowering of the conduction band. Thus, $\text{Ga}_{1-x}\text{In}_x\text{N}_y\text{P}_{1-y}$ may be a suitable material for the emitter and/or collector of a HBT because the conduction-band offset could be made to be zero.⁴ In particular, it can be applied to the tunnel-collector HBT.⁵ Until now, there have been few reports on nitrogen incorporation into $\text{Ga}_{1-x}\text{In}_x\text{P}$. In this letter, we report the optical and electrical properties of bulk $\text{Ga}_{1-x}\text{In}_x\text{N}_y\text{P}_{1-y}$, which is lattice matched to GaAs(001) substrates when $(x-0.48)=2.8y$.

All the samples used in this study were grown on (100) GaAs semi-insulating substrates by gas-source molecular-beam epitaxy (MBE) using elemental Ga and In, thermally cracked arsine (AsH_3), and phosphine (PH_3), and a rf plasma nitrogen radical beam source. Elemental Si was the *n*-type dopant. After removing the surface oxide of the GaAs substrate at 620 °C under an As_2 flux, a 100-nm-thick GaAs buffer layer was grown. Then, the substrate temperature was lowered to the growth temperature, between 380 and 480 °C, and a N plasma was ignited. Growth was monitored by reflection high-energy electron diffraction. Undoped, 235-nm-thick $\text{Ga}_{1-x}\text{In}_x\text{N}_y\text{P}_{1-y}$ layers ($y=0\%–2.3\%$) were grown for optical studies, and Si-doped, 700-nm-thick $\text{Ga}_{1-x}\text{In}_x\text{N}_y\text{P}_{1-y}$ layers were grown for electrical transport studies.

Rapid thermal annealing (RTA) was carried out at different temperature for 10 s in a 100% N_2 ambient. High-resolution x-ray rocking curve measurements were performed using a Phillips x-ray diffractometer. Photoluminescence (PL) measurements were carried out at 10 K by mounting the samples on a cold finger in a liquid He cryostat and using the 514.5 nm line of an Ar^+ laser as the

excitation source. A GaAs photomultiplier tube was used to detect the signal at the exit of a 50 cm monochromator through an amplifier.

The indium composition was determined by dynamical-theory simulations of the measured x-ray rocking curves on the $\text{Ga}_{1-x}\text{In}_x\text{P}$ calibration sample grown on GaAs(001). The nitrogen compositions were determined on bulk $\text{Ga}_{1-x}\text{In}_x\text{N}_y\text{P}_{1-y}$ samples by measuring the magnitude of the shift from $\text{Ga}_{1-x}\text{In}_x\text{P}$ to $\text{Ga}_{1-x}\text{In}_x\text{N}_y\text{P}_{1-y}$. We believe that the competition between In and Ga for the group-III sublattice sites is independent of that between N and P for the group-V sublattice sites. Therefore, we assume nitrogen incorporation does not affect the indium composition. With nitrogen incorporation the PL intensity decreases, and the full width at half maximum (FWHM) increases. Figure 1 shows room-temperature PL spectra for three samples with a N concentration of 0%, 0.2%, and 2%, respectively. The red-shift of the PL peak with nitrogen incorporation indicates a large band-gap bowing. 2% N reduces the band gap by about 220 meV, comparable to the bowing coefficient of $\text{Ga}_{0.90}\text{In}_{0.10}\text{N}_{0.02}\text{As}_{0.98}$.⁶

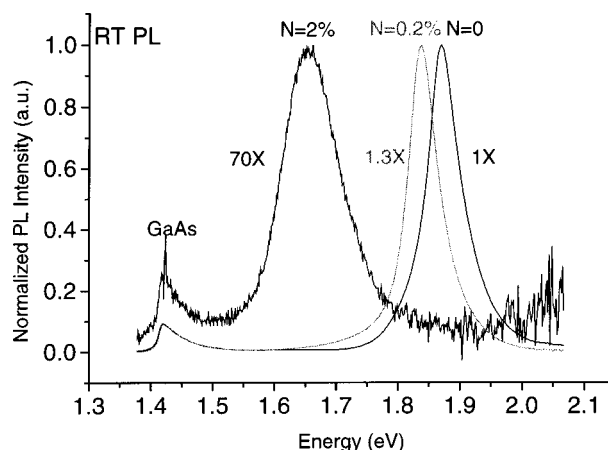


FIG. 1. Normalized room-temperature PL spectra of $\text{Ga}_{0.48}\text{In}_{0.52}\text{N}_y\text{P}_{1-y}$ with different N concentrations.

^{a)}Electronic mail: yghong@ucsd.edu

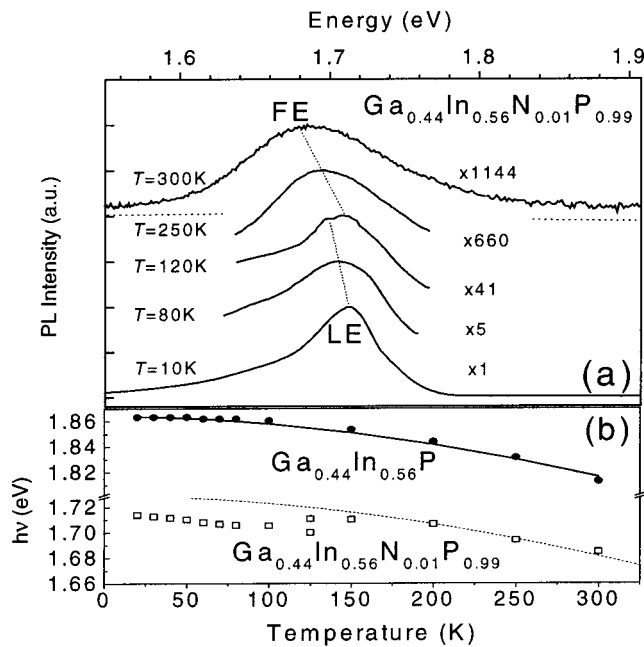


FIG. 2. (a) Normalized PL spectra of $\text{Ga}_{0.44}\text{In}_{0.56}\text{N}_{0.01}\text{P}_{0.99}$ for different temperatures. LE and FE indicate recombination from localized and free excitons, respectively. (b) Temperature dependence of the peak energy, $h\nu$, of PL for $\text{Ga}_{0.44}\text{In}_{0.56}\text{P}$ (full dots) and $\text{Ga}_{0.44}\text{In}_{0.56}\text{N}_{0.01}\text{P}_{0.99}$ (open square). The solid line is fit by the Varshni model and the dashed line is vertically shifted by constant energy from the solid line to check whether it can fit $\text{Ga}_{0.44}\text{In}_{0.56}\text{N}_{0.01}\text{P}_{0.99}$.

Figure 2(a) shows normalized PL spectra at different temperatures for the $\text{Ga}_{0.44}\text{In}_{0.56}\text{N}_{0.01}\text{P}_{0.99}$ sample. At $T = 10$ K only the peak labeled LE (localized excitons) is observed. For $T > 80$ K, a new band FE (free excitons) appears at an energy higher than the LE band and dominates the spectrum up to room temperature without any remarkable line-shape change. We attribute the LE and FE bands to localized and free-exciton recombination, respectively. Temperature-dependent PL spectra show a smooth decrease in the population ratio between LE and FE with increasing temperature T .

It is well known that the temperature dependence of the direct band gap of a semiconductor can be described by the Varshni equation

$$E_g(T) = E_0 - \alpha T^2 / (\beta + T), \quad (1)$$

where E_0 is the band gap at $T = 0$ K and α and β are the Varshni coefficients. The PL peak energy, $h\nu$, is shown as a function of T in Fig. 2(b) for both $\text{Ga}_{0.44}\text{In}_{0.56}\text{N}_{0.01}\text{P}_{0.99}$ and $\text{Ga}_{0.44}\text{In}_{0.56}\text{P}$ samples. The $\text{Ga}_{0.44}\text{In}_{0.56}\text{P}$ PL peak energy can be fitted by the Varshni equation with $E_0 = 1.866$ eV, $\alpha = 1$ meV/K, and $\beta = 1475$ K [solid line in Fig. 2(b)]. The dashed line is vertically shifted by a constant energy from the solid line. In the higher temperature range near room temperature it fits the temperature dependence of the $\text{Ga}_{0.44}\text{In}_{0.56}\text{N}_{0.01}\text{P}_{0.99}$ sample, but in the lower temperature range the $\text{Ga}_{0.44}\text{In}_{0.56}\text{N}_{0.01}\text{P}_{0.99}$ sample exhibits an inverted S-shaped phenomenon. This phenomenon is similar to that observed in GaNAs (Ref. 7) and GaInNAs,⁸ and it is due to N-related localized states. At low T , carriers occupy preferentially these states in the band gap, whereas at high T they are thermally activated to the conduction band. Thus, the nonmonotonous behavior in the $\text{Ga}_{0.44}\text{In}_{0.56}\text{N}_{0.01}\text{P}_{0.99}$ band

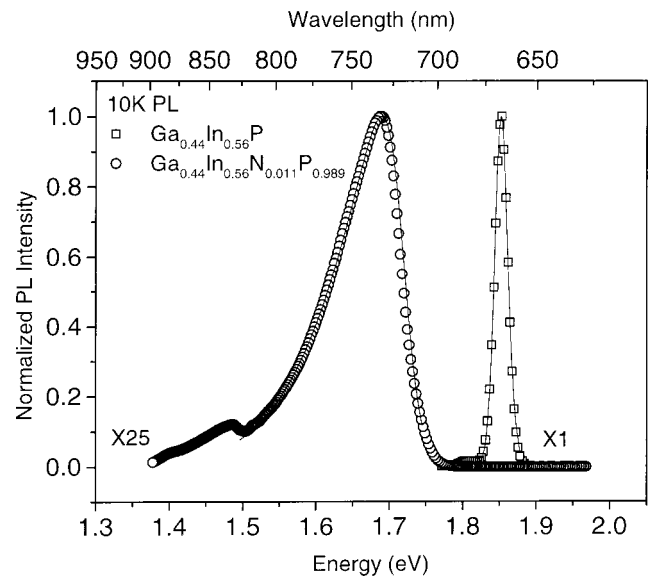


FIG. 3. Low-temperature 10 K PL spectrum of samples $\text{Ga}_{0.44}\text{In}_{0.56}\text{N}_{0.011}\text{P}_{0.989}$ (open circles) and $\text{Ga}_{0.44}\text{In}_{0.56}\text{P}$ (open square).

gap suggests a carrier redistribution between localized and extended states. The carrier freeze-out persists up to $T = 80$ K.

Low-temperature (10 K) PL shows a significant line-shape difference between the N-free $\text{Ga}_{0.44}\text{In}_{0.56}\text{P}$ and nitrogenated $\text{Ga}_{0.44}\text{In}_{0.56}\text{N}_{0.011}\text{P}_{0.989}$ sample, as shown in Fig. 3. The nitrogen-containing sample has an asymmetric PL line shape with a large low-energy tail, from the presence of N-related localized states. This low-energy tail is also present in GaInNAs epilayers⁹ and other semiconductor alloys.^{10,11} The microscopic origins of the low-energy tail could be due to the N composition (and conduction-band edge) fluctuation. The number and potential depth of the carrier trapping centers increases with N concentration. These N isoelectronic traps also have a strong effect on the electron transport properties as described below.

To investigate the electron transport properties of $\text{Ga}_{0.48}\text{In}_{0.52}\text{N}_y\text{P}_{1-y}$, Si-doped samples were grown with the same Si flux but different N_2 flow rates. Hall measurements show decreased electron concentration and mobility with increasing N concentration, as shown in Fig. 4. Incorporation of 0.5% nitrogen decreases electron mobility from 406 to 51 $\text{cm}^2/\text{V s}$. The rapid decrease of electron mobility in $\text{Ga}_{0.48}\text{In}_{0.52}\text{N}_y\text{P}_{1-y}$ is very similar to that of GaInNAs, which could be caused by intrinsic defects or scattering due to the effects of local strain associated with nitrogen incorporation.¹² Furthermore, the electron concentration of $\text{Ga}_{0.48}\text{In}_{0.52}\text{N}_y\text{P}_{1-y}$ decreases with increasing N content, which could indicate increasing N-related electron traps.

The temperature-dependent Hall measurements provided additional insight. The electron mobility of $\text{Ga}_{0.48}\text{In}_{0.52}\text{P}$ is limited by phonon scattering in the high-temperature region and by ionized impurity scattering in the low-temperature region. In contrast, the electron mobility of the N-containing $\text{Ga}_{0.48}\text{In}_{0.52}\text{N}_{0.012}\text{P}_{0.988}$ sample shows little temperature dependence, which indicates a different scattering mechanism. The N incorporation introduces highly localized isoelectronic traps in $\text{Ga}_{0.48}\text{In}_{0.52}\text{P}$, as a consequence of the difference in the electronegativity, size, and pseudopotential be-

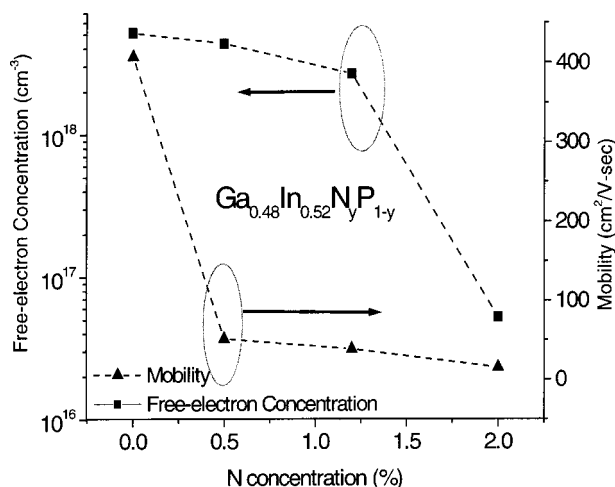


FIG. 4. Nitrogen effect on free-electron concentration and mobility of as-grown samples.

tween the isoelectronic impurity N and host atom P. Such traps are characterized by a potential that varies with distance much faster than the Coulomb potential of shallow donors.¹³ These isoelectronic levels trap free electrons; thus, scattering by such isoelectronic traps is less temperature dependent.¹⁴

In order to improve the sample quality, we annealed the samples for 10 s under N_2 ambient at different rapid thermal annealing temperatures. For the $Ga_{0.48}In_{0.52}P$ sample, the free-electron concentration decreases gradually from 5.1×10^{18} to $1.1 \times 10^{18} \text{ cm}^{-3}$ (see Fig. 5) as the RTA temperature increases to 800°C , which could be due to autocompensation from the amphoteric behavior of Si. At higher temperatures, an increasing number of Si atoms would occupy P sites. On the other hand, the electron concentration of $Ga_{0.48}In_{0.52}N_{0.005}P_{0.995}$ decreases much more rapidly, from 4.4×10^{18} to $8.0 \times 10^{16} \text{ cm}^{-3}$, although no structural degra-

dation was observed by x-ray measurements even for the 800°C annealed sample, as shown in the inset of Fig. 5.

The monotonic decrease of the free-electron concentration of Si-doped $Ga_{0.48}In_{0.52}N_yP_{1-y}$ with annealing temperature is contrary to the expectation that annealing should anneal out point defects, as in the behavior of the hole concentration of Be-doped $Ga_{0.892}In_{0.108}N_{0.011}As_{0.989}$, which increases as a function of annealing temperature up to 750°C .⁶ Recently Yu *et al.* proposed a model of mutual passivation between Si and N,¹⁵ that is, Si is passivated by N, and vice versa, through the formation of Si–N pairs. N is more electronegative than P (Pauling electronegativities of N and P being 3.04 and 2.19, respectively); thus, N has a tendency to bind the free valence electron of Si. When $Ga_{0.48}In_{0.52}N_yP_{1-y}$ is grown at a relatively low temperature ($\sim 450^\circ\text{C}$) by MBE, Si atoms are randomly distributed in the Ga sublattice sites. During RTA at high temperatures, Si atoms have enough thermal energy to diffuse to be near N to form Si–N pairs. This passivation process results in a significant drop in the free-electron concentration in N-containing $Ga_{0.48}In_{0.52}N_{0.005}P_{0.995}$.

In summary, nitrogen incorporation dramatically reduces the $Ga_{1-x}In_xP$ band gap. The PL peak energy exhibits an inverted S-shaped dependence with temperature, indicating the presence of localized states, which dominate the radiative recombination processes at low temperatures. Isoelectronic N traps have strong effects not only on the optical properties but also on the electron transport properties. Hall measurements show a decreasing free-electron concentration and mobility with increasing N concentration. High-temperature RTA results in a significant drop in the free-electron concentration in N-containing $Ga_{0.48}In_{0.52}N_{0.005}P_{0.995}$, indicating that Si is passivated by N, due to the much larger electronegativity of N, through the formation of Si–N pairs.

This work was supported by the National Renewable Energy Laboratory (Grant No. AAD-9-18668-07).

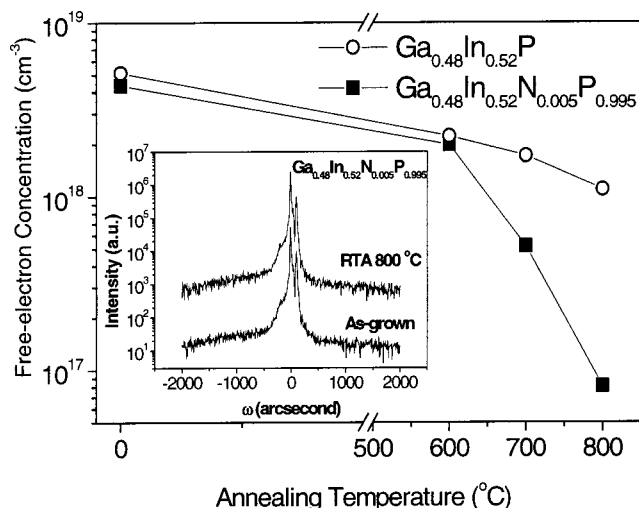


FIG. 5. Free-electron concentrations of Si-doped $Ga_{0.48}In_{0.52}N_{0.005}P_{0.995}$ and $Ga_{0.48}In_{0.52}P$ samples. Results were obtained by Hall-effect measurements as a function of rapid thermal annealing temperature. The inset is the x-ray result of as-grown and 900°C annealed Si-doped $Ga_{0.48}In_{0.52}N_{0.005}P_{0.995}$, respectively.

¹K. A. Bertness, S. R. Kurtz, D. J. Friedman, A. E. Kibbler, and J. M. Olson, Appl. Phys. Lett. **65**, 989 (1994).

²D. A. Ahmari, G. Raghavan, Q. J. Hartmann, M. L. Hattendorf, M. Peng, and G. E. Stillman, IEEE Trans. Electron Devices **46**, 634 (1999).

³W. Shan, W. Walukiewicz, J. W. Ager III, E. E. Haller, J. F. Geisz, D. J. Friedman, J. M. Olson, and S. R. Kurtz, Phys. Rev. Lett. **82**, 1221 (1999).

⁴Y. G. Hong, R. Andre, and C. W. Tu, J. Vac. Sci. Technol. B **19**, 1413 (2001).

⁵R. J. Welty, Y. G. Hong, H. P. Xin, K. Mochizuki, C. W. Tu, and P. M. Asbeck, Proceedings of the IEEE/Cornell Conference on High Performance Devices, Piscataway, NJ, (2000), pp. 33–40.

⁶H. P. Xin, C. W. Tu, and M. Geva, Appl. Phys. Lett. **75**, 1416 (1999).

⁷K. Uesugi, I. Suemune, T. Hasegawa, T. Akutagawa, and T. Nakamura, Appl. Phys. Lett. **76**, 1285 (2000).

⁸M.-A. Pinault and E. Tournie, Appl. Phys. Lett. **78**, 1562 (2001).

⁹R. A. Mair, J. Y. Lin, H. X. Jiang, E. D. Jones, A. A. Allerman, and S. R. Kurtz, Appl. Phys. Lett. **76**, 188 (1999).

¹⁰D. Oudjaout and Y. Marfaing, Phys. Rev. B **41**, 12096 (1990).

¹¹A. Ait-Ouali, R.-F. Yip, J. L. Brebner, and R. A. Masut, J. Appl. Phys. **83**, 3153 (1998).

¹²J. F. Geisz, D. J. Friedman, J. M. Olson, S. R. Kurtz, and B. M. Keyes, J. Cryst. Growth **195**, 401 (1998).

¹³R. A. Faulkner, Phys. Rev. **175**, 991 (1968).

¹⁴W. Walukiewicz, J. Lagowski, L. Jastrzebski, P. Rava, M. Lichtensteiger, C. H. Gatos, and H. C. Gatos, J. Appl. Phys. **51**, 2659 (1980).

¹⁵K. M. Yu, W. Walukiewicz, J. Wu, D. E. Mars, D. R. Chamberlin, M. A. Scarpulla, O. D. Dubon, and J. F. Geisz, Nature Materials **1**, 185 (2002).